Geoscience Frontiers 15 (2024) 101852

Contents lists available at ScienceDirect

Geoscience Frontiers

journal homepage: www.elsevier.com/locate/gsf

Research Paper

Regional trends and petrologic factors inhibit global interpretations of zircon trace element compositions

Nick M.W. Roberts [a,*], Christopher J. Spencer [b], Stephen Puetz [c], C. Brenhin Keller [d], Simon Tapster [a]

[a] Geochronology and Tracers Facility, British Geological Survey, Nottingham NG12 5GG, UK
[b] Department of Geological Sciences and Geological Engineering, Queen's University, Kingston, Ontario, Canada
[c] 475 Atkinson Dr, Suite 704, Honolulu, HI 96814, USA
[d] Department of Earth Sciences, Dartmouth College, Hanover, New Hampshire, USA

ARTICLE INFO

Article history:
Received 22 March 2024
Revised 16 April 2024
Accepted 7 May 2024
Available online 9 May 2024
Handling Editor: M. Santosh

Keywords:
Detrital zircon
Trace elements
Secular change
Eu anomaly
Crustal thickness

ABSTRACT

The trace element composition of zircon reveals information about the melt that they are derived from, as such, detrital zircon trace element compositions can be used to interrogate melt compositions, and thus the evolution of the continental crust in time and space. Here, we present a global database of detrital zircon compositions and use it to test whether average global trends for five common petrogenetic proxies truly represent secular changes in continental evolution. We demonstrate that the secular trend is broadly comparable across continental regions for Ti-in-zircon temperatures, but for other trace element ratios interrogated, secular trends are highly variable between continental regions. Because trace element ratios result from multiple petrologic variables, we argue that these petrogenetic proxies can be overinterpreted if projected to global geologic processes. In particular, we caution against the interpretation of crustal thickness from trace elements in zircon, and we argue that our results negate current hypotheses concerning secular changes in crustal thickness.

1. Introduction

Due to its physical and chemical resilience, zircon remains the most popular mineral for studying the long-term evolution of Earth's continental crust (e.g. Castillo et al., 2022; Zhang et al., 2023; Pereira et al., 2024). Detrital zircon datasets have broad spatial and temporal coverage of the continents, and beyond the use of sediment provenance, are commonly used to understand secular changes in magmatic and metamorphic processes (e.g. Dhuime et al., 2012; Roberts and Spencer, 2015). In the last few years, there has been a significant rise in the use of zircon trace element compositions to track secular change in continental evolution on both regional (Brudner et al., 2022; Dong et al., 2022, 2023; Jaramillo et al., 2022; Lei et al., 2022; Liu et al., 2022, 2023; Moghadam et al., 2022; Wang et al., 2022; Zeng et al., 2022; Hu et al., 2023a, b; Li et al., 2023; Wu et al., 2023; Xiong et al., 2023; Cheng et al., 2024; Sundell et al., 2024) and global scales (McKenzie et al., 2018; Balica et al., 2020; Tang et al., 2021b; Verdel et al., 2021; Paulsen et al., 2022; Moreira et al., 2023). This rise is driven by the use of trace element proxies as petrogenetic indicators, for example, Ti as a function of temperature (Watson et al., 2006) and Eu/Eu* as a proxy for crustal thickness (Tang et al., 2021a).

To date, global detrital zircon trace element compilations have arguably not been extensive, generally comprising <10,000 records, and biased towards certain regions (e.g. McKenzie et al., 2018; Balica et al., 2020; Paulsen et al., 2021; Tang et al., 2021b; Verdel et al., 2021; Triantafyllou et al., 2023). This begs the important question, to what extent are these datasets representative of global processes? For Hf isotopes, Sundell and Macdonald (2022) conducted a study using the Puetz et al. (2021) database (n = 165,111) into regional variance and demonstrated that global trends reflect the evolution of specific orogens, which do not necessarily reflect contemporaneous secular evolution of global processes. Furthermore, the direct use of most petrogenetic proxies is often heavily caveated and/or shown to be problematic (e.g. Triantafyllou et al., 2023), but these issues tend not to deter their use (e.g. Wu et al., 2023).

Here, we present an updated literature compilation of trace element compositions of detrital zircon, comprising ~47,000 filtered analyses (n = ~77,000 unfiltered). The aim of this contribution is threefold: (1) present an updated comprehensive global compilation that is open access and comprises thorough metadata records; (2) test global trends in common petrogenetic proxies to demon-

* Corresponding author.
E-mail address: nirob@bgs.ac.uk (N.M.W. Roberts).

https://doi.org/10.1016/j.gsf.2024.101852
1674-9871/

strate the potential effects of regional bias; and (3) comment on the robustness of the most common petrogenetic proxies in light of our findings and incorporating known issues and caveats.

2. Methods and data

Trace element compositions of zircon were collated from 112 literature sources, comprising 562 individual samples, and 77,127 individual records. We aimed to provide a comprehensive coverage of the current literature; in general, most omitted publications are scant in metadata or contain very few individual records. Correlative age data were collected for a subset of data, generally where they were provided in the same format and/or in the same data tables. Compiled metadata include location information: continent, country, location, and GPS coordinates in a common UTM format. The locations are taken from the original sources, and where not provided, estimated from published map figures. The database is provided in full at https://figshare.com/s/89d01010d6a7ba4c9592.

For our analysis of global trends, we have filtered the data for discordance, inclusions, and anomalous values, and provided a 'preferred age' for each record. Trends of elemental concentration or element ratio with age are shown as means, binned at 100 Myr intervals, and calculated using a weighted bootstrap resampling method following Keller and Schoene (2012). This approach helps alleviate sampling bias by assigning each sample a resampling probability that is inversely correlated to spatial and temporal sample density (Keller and Schoene, 2012). Details of filtering, choice of age, and plotting are described in the Supplementary Data Text. Additional figures comprising alternative methods for plotting secular trends are also included in the Supplementary Files. Ti-in-zircon temperatures use the calibration of Ferry and Watson (2007) and assume fixed silica and titanite activities of 1.0 and 0.5, respectively (Schiller and Finger, 2019). Eu/Eu* is calculated using chondrite normalised (McDonough and Sun, 1995) Eu/$\sqrt{}$(Sm*Gd).

3. Results

Our filtered database comprises 47,182 records and covers all continents; however, there is sampling bias towards certain regions, with Africa and South America having disproportionately low abundance (Fig. 1a). The records span Earth's history with increasing density through time (Fig. 1b). In Fig. 1c it can be seen that the data have broad global coverage, but with significant continental areas still missing any records. Any hypotheses regarding global processes should be aware of these discrepancies in global coverage, even if attempts are made to account for regional bias with statistical methods (e.g. Keller and Schoene, 2012). Noting the still existent regional bias in the database, it is still somewhat more extensive than those used previously (e.g. Balica et al., 2020; Tang et al., 2021b; Verdel et al., 2021; Paulsen et al., 2022).

In Figs. 2 and 3 we plot five individual proxies, modelled Ti-in-zircon temperatures, Eu/Eu*, Yb/Gd, Th/Yb, and U/Yb. We plot both average global trends using the weighted bootstrap approach and compare the data with previous publications (plotted using the same method), and we plot individual trends for the four continents with large temporal data coverage that dominate the current database (Antarctica, Asia, North America, and Oceania). Alternative statistical methods of displaying these trends are demonstrated in the Supplementary Information (Supplementary Data Figs. S1 and S2).

4. Discussion

4.1. Robust trends in thermometry?

The Ti-based zircon thermometer has long been considered robust, but it is well known that Si and Ti activities must be constrained to achieve accurate temperature estimates (e.g. Schiller and Finger, 2019). The pressure dependence of this thermometer has been considered negligible, although recent work implies a subtle pressure effect that needs to be considered for high-pressure zircon growth especially (Crisp et al., 2023). Temperature estimates from single magmatic rocks often exhibit a large range, implying zircon crystallisation over a protracted temperature range (Ickert et al., 2011), and/or diffusion (Bloch et al., 2022). As such, any detrital zircon estimate has to consider that a single temperature datum may relate to a snapshot of a broader magmatic and cooling history. Regarding secular trends in temperatures derived from detrital zircon, these have to be constructed using single choices of Si and Ti activities and pressure and thus may average out some variation that would be exhibited by the true temperature range.

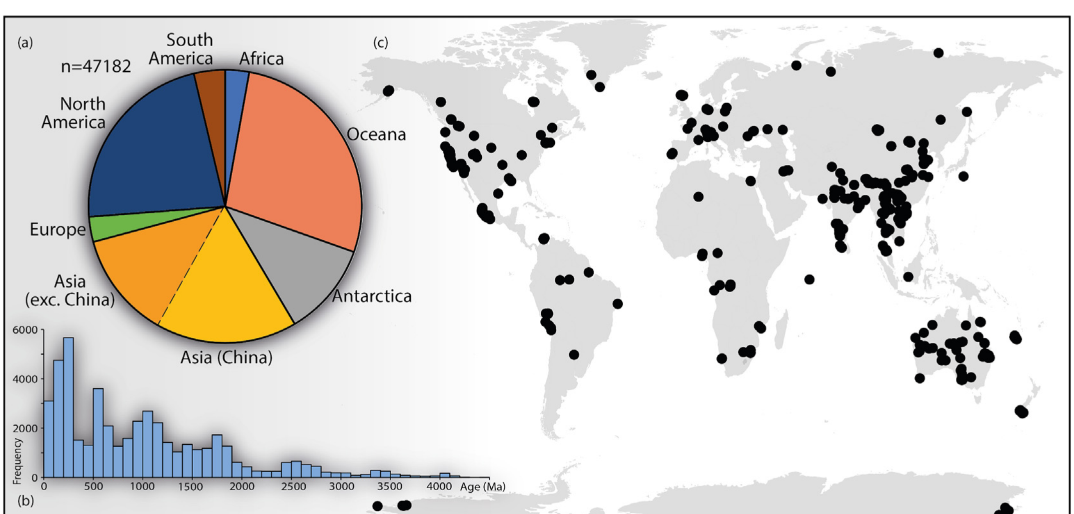

Fig. 1. (a) Pie chart showing the density of detrital zircon per continent (filtered dataset). (b) Histogram (100 Myr binwidth) of the U-Pb ages of the filtered detrital zircon dataset. (c) World map showing locations of all samples.

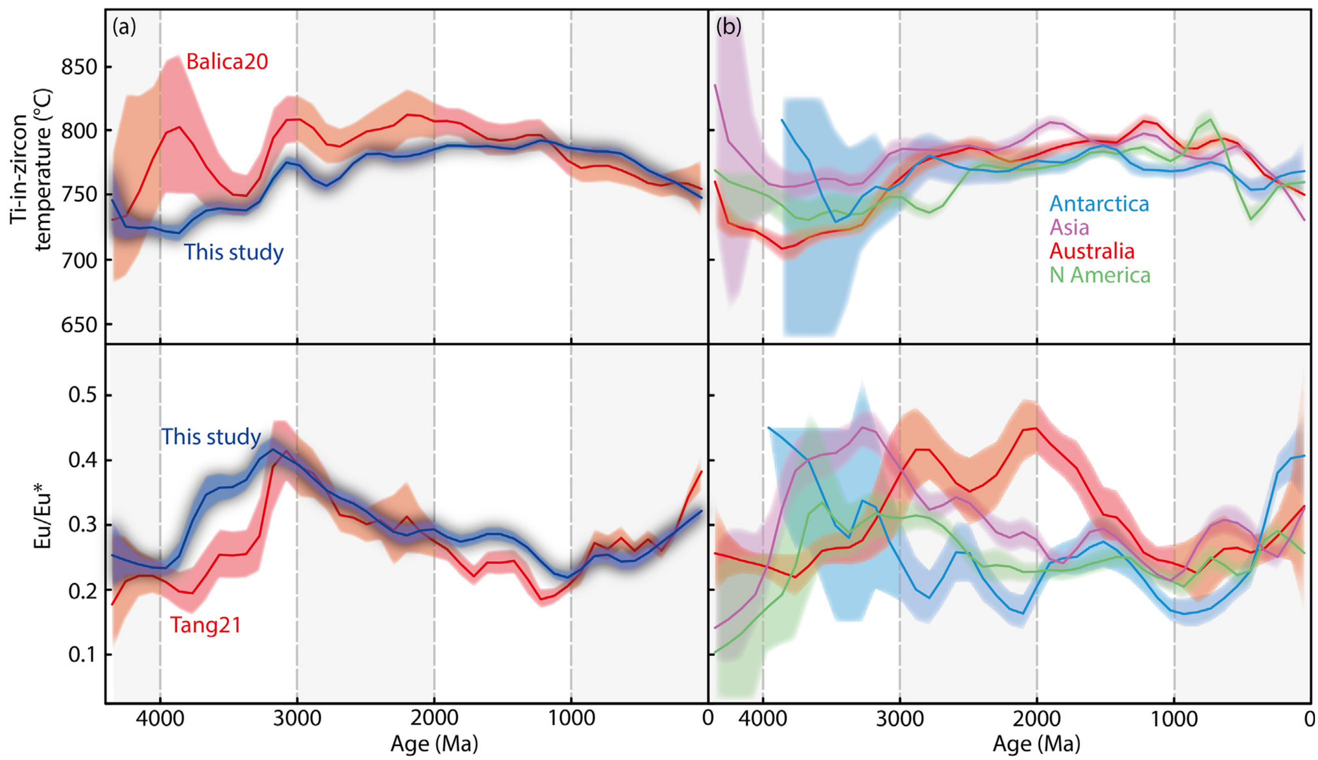

Fig. 2. (a) Modelled Ti-in-zircon temperatures and Eu/Eu* for our global detrital zircon database compared to previous databases (Balica et al., 2020; Tang et al., 2021b); uncertainty envelopes ignore the calibration of the Ti thermometry and are based on fixed Si and Ti activities of 1.0 and 0.5, respectively. (b) Continental-scale comparison of our detrital zircon database comparing trends from four continents. All plots are shown as weighted bootstrap means with error bands representing 2 standard errors of the mean.

Based on a detrital zircon compilation with broad global coverage, Balica et al. (2020) noted “A distinctive increase from 700–800 °C pre-3.2 Ga followed by a gradual decrease since then”. Within our larger dataset, we see a similar increase up to ca. 3.0 Ga, but rather than decreasing, the global trend has a marginal increase up to ca. 1.2 Ga. Only after ca. 1.2 Ga does the trend decrease, and particularly rapidly after ca. 0.7 Ga. Assessing the continent-specific trends, we can see that pre-3.2 Ga is varied, with large uncertainties owing to sparse data coverage; however, overall there is a marked increase from values pre- and post- 3 Ga. From ca. 3 Ga to 1 Ga, values for each continent vary, but overall show a broad stability with only minor variation. All continents exhibit lower temperatures in the Phanerozoic, with the onset of decreasing values varying between continents. Based on these observations, the following observations likely represent global processes: (1) an increase in modelled temperatures through the early Archean up to ca. 3 Ga; (2) consistent modelled temperatures (in the range of 750–800 °C) from ca. 3 Ga to 1 Ga; and (3) lower modelled temperatures into the Phanerozoic (ca. 750 °C). We note that these absolute values depend on the choice of Si and Ti activities, but the scale of increasing and decreasing modelled temperatures is likely independent of these activities.

Balica et al. (2020) argued that the apparent change in temperature at ~3.2 Ga “must mark the change from eutectic of the albite-anorthite-quartz system towards progressively higher dehydration melting of biotite and amphibole-bearing rocks”. In contrast, Verdel et al. (2021) simply relate higher zircon temperatures throughout the Proterozoic to higher crustal temperatures. If Ti-in-zircon simply recorded the highest primary temperatures of a magmatic rock, then the secular changes may indeed record changing reactions and/or geotherms. However, zircon temperatures in magmatic rocks relate to multiple petrologic variables, including the timing and temperature of zircon saturation during a magma’s evolution, which in turn is related to magma chemistry (*e.g.* Laurent et al., 2022). Thus, secular trends in zircon thermometry likely result from multiple underlying variables that also exhibit secular changes; these include most obviously the changing geochemistry of igneous rocks (*i.e.* Keller and Schoene, 2012), but may also include changing cooling rates; the latter may be influenced by crustal thickness, but will also depend on variables such as radiogenic heating and rate of erosion. Deconvolving the contributions of different processes that led to the apparent global secular pattern is not trivial; however, we demonstrate using a global database of intermediate-felsic igneous rock compositions (Fig. 4) that secular changes in magmatic composition, both the Zr abundance and M (relating to alkali content), likely have a controlling factor. These variables will change the saturation and growth history of zircon in magmatic rocks, and thus, in turn, will also be reflected in Ti-based zircon thermometry.

Regarding the cause of such secular changes in magmatic rocks, increasing Zr contents of basalts have been linked to: (1) decreasing mantle temperatures and the associated decrease in degrees of mantle melting (Keller and Schoene, 2018), along with (2) a potential increase in enriched mantle sources after *ca.* 2 Ga (Condie et al., 2022b). Granitoids, the dominant source of detrital zircon, are ultimately derived from mantle-derived basalts (senso lato) via a variety of mechanisms, and broadly echo the trend of basalts (Condie et al., 2024). A significant increase in Zr contents of granitoids during the mid-Proterozoic, along with other ‘A-type’ traits, has been linked to an increase in hot and dry granite formation during this time (Roberts et al., 2023).

4.2. Eu/Eu*, a robust ‘barometer’?

There has been a substantial effort in recent years to use whole-rock geochemical signatures of igneous rocks to estimate the depth

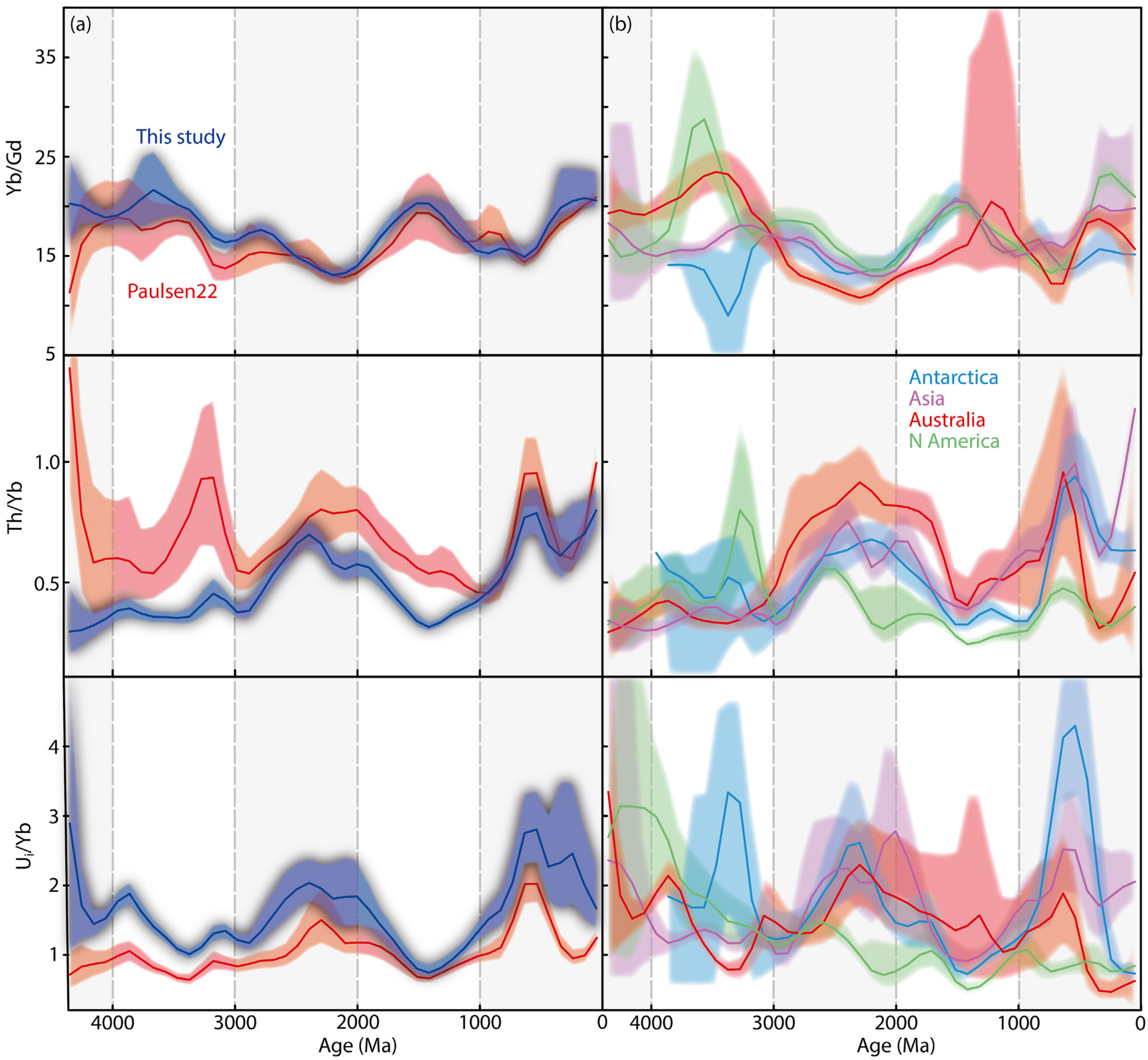

Fig. 3. (a) Yb/Gd, Th/Yb, and U/Yb for our global detrital zircon database compared to a previous database (Paulsen et al., 2022). (b) Continental-scale comparison of our detrital zircon database comparing trends from four continents. All plots shown as weighted bootstrap means with error bands representing 2 standard errors of the mean. Note that for our database, U/Yb incorporates age-corrected U concentrations (U_i/Yb).

of melting and/or the thickness of the crustal column, a field that has recently been coined 'chemical mohometry' (Luffi and Ducea, 2022). Many geochemical signatures rely on the contrasting behaviour between garnet and plagioclase which are stable at deep and shallow crustal levels, respectively (e.g. Alonso-Perez et al., 2009). Well-constrained trends between average arc thicknesses and whole-rock La/Yb and Sr/Y have been demonstrated (Chapman et al., 2015; Profeta et al., 2015). Tang et al. (2021a) argued that zircon could be used in the same manner, suggesting that if Eu anomalies reflect plagioclase fractionation, then these could equally be linked to crustal thickness. Their proxy for crustal depth links Eu/Eu* to whole-rock La/Yb, and relies on previous constraints for thickness from La/Yb. Tang et al. (2021b) investigated Eu anomalies of a global detrital zircon dataset, demonstrating that the greatest negative anomalies – and thus, lower crustal thicknesses, occurred in a period known as Earth's 'Middle Age' (1.8–0.8 Ga). Our average global mean (Fig. 2) replicates the broad overall trend of decreasing then increasing values between 3 Ga and 0 Ga; however, there is a critical difference that is pertinent to the conclusions of Tang et al. (2021b). Specifically, the minima in that study broadly span the Mesoproterozoic eon (1.6–1.0 Ga), whereas, in our dataset, the minima are offset to younger ages (~1.0 Ga to 0.7 Ga). Examining the continent-based trends in Fig. 2, we argue there is even more cause for concern. Although all continents seem to exhibit low values between ca. 1.2 Ga and 0.5 Ga, data before ca. 1.5 Ga are highly varied, with significant variation between the continents throughout the Archean. As such, we question the validity of the averaged global trend as representing global secular change. A direct correlation between low Eu anomalies and Earth's Middle Age is negated (c.f., Tang et al., 2021b).

Building on other previous studies, we highlight several potential problems with this proxy: (1) the statistical treatment is not robust, relying on an indirect correlation through a whole-rock

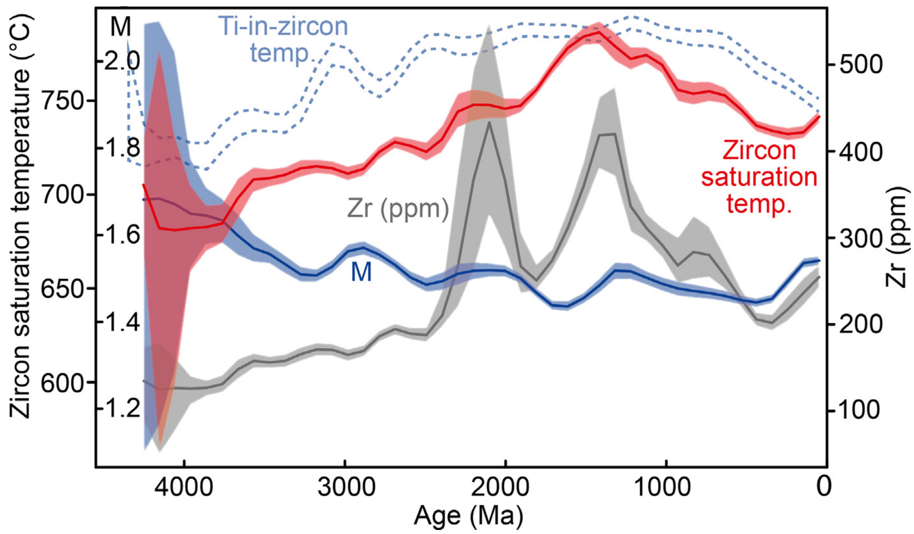

Fig. 4. Comparison of whole-rock and zircon-based temperatures. The dashed trend is modelled Ti-in-zircon thermometry from the global detrital zircon database, as in Fig. 2. Red, grey and blue trends are based on the global igneous felsic rock compilation of Gard et al. (2019) filtered to 45%–80wt.% SiO_2, and demonstrate the zircon saturation temperatures calculated using the equation of Boehnke et al. (2013), Zr abundance (ppm) and M value, respectively. All trends shown as weighted bootstrap means with error bands representing 2 standard errors of the mean.

proxy (see Supplementary Data Text for further discussion); (2) Eu anomalies are partially controlled by temperature and redox (Trail et al., 2012; Yakymchuk et al., 2023); (3) plagioclase and garnet stability in the crust varies with composition, conditions (i.e. water content) and geothermal gradient (Tamblyn et al., 2022; Triantafyllou et al., 2023); and, (4) Eu/Eu* will be imparted from the magma source, with contamination of magmas altering the primary Eu signature (Bell and Kirkpatrick, 2021). Both Triantafyllou et al. (2023) and Yakymchuk et al. (2023) cautioned against the use of this proxy for understanding crustal thickness in deep time, and we reiterate those concerns, suggesting that a correlation between Eu/Eu* and crustal thickness is not valid. Furthermore, based on these issues and those outlined with the global trends above, we argue the jury is still out as far as estimates of mid-Proterozoic crustal thickness are concerned.

4.3. HREE-dependant proxies

Several petrogenetic zircon-based proxies use contrasting behaviour of REEs, such as light to heavy or middle to heavy REE, or involve other elements that are mobile/immobile under certain conditions. Commonly used ratios include Th/Yb, U/Yb, La/Yb, and Yb/Gd. Paulsen et al. (2021, 2022) argue that because Th is enriched relative to other elements as the continental crust matures, increasing Th/Yb ratios in zircon can be used as a proxy for evolved magmatism that involves the recycling of older radiogenic crust. U/Yb has variably been used as both a proxy for subduction input and to discriminate continental from oceanic-crust derived zircon (Grimes et al., 2007; Paulsen et al., 2021, 2022; Verdel et al., 2021), owing to the U enrichment from slab-derived fluids during subduction. Yb/Gd is used as a proxy for HREE to MREE enrichment. Since HREE is more compatible with garnet in comparison to most other major igneous minerals, the presence of garnet during zircon crystallisation strongly controls the resulting Yb/Gd ratios. Given the pressure dependence on garnet stability, Yb/Gd has been used as a broad proxy for crustal thickness (Paulsen et al., 2021, 2022). Similarly, Verdel et al. (2021) used Lu/Nd as a proxy for HREE/LREE, with their overall premise of low ratios equalling the involvement of thick continental crust being comparable. La/Yb is used as a proxy for LREE to HREE enrichment and equally is related to crustal thickness due to the effect of garnet ± amphibole on Yb abundance in zircon (Chapman et al., 2015; Balica et al., 2020).

The use of the above-mentioned ratios as proxies is hindered by a variety of factors. Specific to U, is the fact that U incorporation in zircon likely has a redox control, even if minor (Loucks et al., 2018). Four important factors are more generally relevant to all of these proxies and in fact most elemental ratios in zircon: (1) Co-crystallisation of other mineral phases is not always considered. For example, sequestration of HREE in garnet is argued as a factor strongly influencing all of the aforementioned ratios, yet Th incorporation in monazite or allanite is not considered for Th/Yb. (2) The stability of phases that sequester the elements of interest depends on multiple variables beyond pressure, such as temperature and water content (e.g. Tamblyn et al., 2022; Triantafyllou et al., 2023; Roberts et al., 2024). (3) An important but typically ignored problem, particularly relevant for ratios involving a HREE (i.e. Yb), is that zircon itself has a markedly high partition coefficient for Yb (Claiborne et al., 2018) – orders of magnitude higher than that of most other igneous minerals. Therefore, as soon as zircon starts to crystallise, HREE in the melt will become depleted, and thus the ratio involving REEs will change through the magmatic history whilst zircon is crystallising/dissolving (Reimink et al., 2020; Zhong et al., 2021). As such, a detrital zircon ratio will be just a snapshot of this complex evolution. (4) Finally, as mentioned above for Eu/Eu*, contamination and assimilation of magmas during their evolution will influence the melt trace element budget. In summary, any single apparent secular trend may reflect multiple processes, and assuming a control by pressure-dependant mineral phases is likely a significant misinterpretation of the data.

4.4. HREE-dependant trends

Paulsen et al. (2022) described three peaks in Th/Yb in their global dataset, at 3.2 Ga, 2.5–1.9 Ga, and 0.5 Ga, and a period of lower values throughout Earth's Middle Age. Excluding the ca. 3.2 Ga peak, the averaged global trend of our dataset also records these peaks and troughs. Examining the trends in the continent-specific data, it can be seen that all continents exhibit higher values in the broad period ca. 2.7–1.7 Ga, and again at ca. 0.7–0.5 Ga. Minima vary between the continents but overlap in the broad region of 1.5–0.8 Ga. As noted by Paulsen et al. (2022), these periods of elevated Th/Yb ratios broadly match increases in recycling of older crust as determined by Sr and Hf isotope data. However, we highlight that higher ratios in the late Archean to early Paleoproterozoic do not overlap with Columbia supercontinent formation at ca. 2.0–1.6 Ga, but do overlap with the period ca. 2.4–2.2 Ga that comprises lower records of tectonic and magmatic activity (Condie et al., 2022a). This observation questions a direct link between Th/Yb ratios and orogenesis, beyond the general issues we highlight above with these petrogenetic proxies.

Paulsen et al. (2022) highlighted that peaks in U/Yb correlated with their peaks in Th/Yb, and we see comparable overlap between Th/Yb and U/Yb in our averaged global mean trends. Using the continent-specific data to examine the importance of these trends, we note that U/Yb is somewhat more variable between continents than Th/Yb. Overall, peaks fall between ca. 2.7 Ga to 1.7 Ga, and ca. 0.7–0.5 Ga (with data > 3 Ga being highly variable); however, North America does not match the global average, exhibiting a different periodicity of peaks and troughs. The reason for the mismatch between continents may be a result of different tectonic settings dominating different regions, i.e. the Grenville orogens being extensive in North America, and the Pan-African orogens extending through Africa into Asia (India), Australia, and Antarctica; however, this still infers a link between tectonic setting, orogenesis and these trace element proxies, which remains to be robustly tested.

Paulsen et al. (2022) demonstrated a broad inverse relationship between Yb/Gd and their other proxies for crustal thickness/maturity (Th/Yb and U/Yb). In our expanded database, this inverse relationship can be seen on a broad level, but there is some offset between the peaks and troughs. Examining the continent-specific data, we see correlative behaviour between three of the four continents shown, with Antarctica clearly having high variability during the Mesoproterozoic. Trends pre-3 Ga are highly variable. If Yb/Gd truly represents the presence or absence of garnet during zircon crystallisation, then at face value, the trends imply minimal garnet presence at ca. 1.5 Ga and ca. 0.5–0 Ga, and maximum garnet presence at ca. 2.5–2.0 Ga, and ca. 1.0–0.6 Ga. However, an important observation is that these trends are uncorrelated to those defined by Eu anomalies, which Tang et al. (2021a) argue are also dictated by the role of plagioclase versus garnet during crystallisation.

5. Implications for secular change

As identified by Sundell and Macdonald (2022) for Hf isotope data of large detrital zircon datasets, the results will be dominated by the influence of large orogens and crust-forming events. Not all orogens are characterized by the same geodynamic configuration or resultant isotopic signatures (Spencer et al., 2013), with accretionary versus collisional orogens having different architectures in terms of crustal recycling, crustal thickness, and geothermal gradients; all these variables will influence zircon trace elements compositions in some way. As such, averaged global trends reflect the average of the active orogenesis through time, and specific orogens may record secular changes in continental evolution at different times in different ways. An example of this is the zircon Eu anomaly, which is clearly highly divergent during the Paleoproterozoic, even though this time period is dominated by the formation of the Columbia supercontinent across all continents examined.

We have only addressed a subset of the numerous trace element proxies used hitherto. As discussed above, each proxy is controlled by multiple competing variables such as redox, co-crystallising mineral assemblage, initial melt composition, and extent of crystal fractionation. None of which are a single function of the pressure of melting or crystallisation. As such, the use of zircon trace element proxies for determining trends in crustal composition or thickness should be used with great caution, or, should at least only be applied to igneous populations (i.e. Moreira et al., 2023). Given the multiple variables behind these trace element ratios, it is perhaps no surprise that correlations between some of the proxies are poor (see Supplementary Data Fig. S3).

6. Conclusions

We present a literature database of ~72,000 detrital zircon trace element compositions, which allows comparison between continents, and evaluation of the robustness of average global trends. Whereas some trace elements/ratios are consistent across continents, i.e. Ti-in-zircon temperatures, others are highly variable. In particular, Eu/Eu* is highly variable between different continents, implying that the average global trend does not simply represent secular change in crustal thickness. Most importantly, we argue that because zircon trace element ratios result from the interplay of multiple competing petrologic variables, trace element proxies for crustal composition and thickness are fraught with uncertainties and should be heavily caveated or avoided completely.

CRediT authorship contribution statement

Nick M.W. Roberts: Writing – original draft, Validation, Formal analysis, Data curation, Conceptualization. **Christopher J. Spencer:** Writing – review & editing, Visualization. **Stephen Puetz:** Writing – review & editing, Data curation. **C. Brenhin Keller:** Writing – review & editing. **Simon Tapster:** Writing – review & editing, Investigation.

Data availability

Data and methods associated with this paper are stored and accessible from Figshare: https://figshare.com/s/89d01010d6a7ba4c9592

Declaration of competing interest

The authors declare that they have no known competing financial interests or personal relationships that could have appeared to influence the work reported in this paper.

Acknowledgements

The authors would like to thank Prof. Santosh for his efficient editorial handling, Peter Cawood for his review, and Oscar Laurent and Jesse Reimink for comments on an earlier version. The authors also thank Thea Hinks for sharing code. NR and ST publish with the permission of the Director of the British Geological Survey and are partly supported by funding from the UK Natural Environment Research Council (NE/Y00549/1). ST was supported by NERC Highlight Topic award "FAMOS" (From arc magmas to ores) NE/P01724X/1 (British Geological Survey).

Appendix A. Supplementary data

Supplementary data to this article can be found online at https://doi.org/10.1016/j.gsf.2024.101852.

References

Alonso-Perez, R., Müntener, O., Ulmer, P., 2009. Igneous garnet and amphibole fractionation in the roots of island arcs: experimental constraints on andesitic liquids. Contrib. Mineral. Petrol. 157, 541.
Balica, C., Ducea, M.N., Gehrels, G.E., Kirk, J., Roban, R.D., Luffi, P., Chapman, J.B., Triantafyllou, A., Guo, J., Stoica, A.M., Ruiz, J., 2020. A zircon petrochronologic

view on granitoids and continental evolution. Earth Planet. Sci. Lett. 531, 116005.
Bell, E.A., Kirkpatrick, H.M., 2021. Effects of crustal assimilation and magma mixing on zircon trace element relationships across the Peninsular Ranges Batholith. Chem. Geol. 586, 120616.
Bloch, E.M., Jollands, M.C., Tollan, P., Plane, F., Bouvier, A.S., Hervig, R., Berry, A.J., Zaubitzer, C., Escrig, S., Müntener, O., Ibañez-Mejia, M., 2022. Diffusion anisotropy of Ti in zircon and implications for Ti-in-zircon thermometry. Earth Planet. Sci. Lett. 578, 117317.
Boehnke, P., Watson, E.B., Trail, D., Harrison, T.M., Schmitt, A.K., 2013. Zircon saturation re-revisited. Chem. Geol. 351, 324–334.
Brudner, A., Jiang, H., Chu, X., Tang, M., 2022. Crustal thickness of the Grenville orogen: A Mesoproterozoic tibet? Geology 50, 402–406.
Castillo, P., Bahlburg, H., Fernandez, R., Fanning, C.M., Berndt, J., 2022. The European continental crust through detrital zircons from modern rivers: Testing representativity of detrital zircon U-Pb geochronology. Earth-Sci. Rev. 232, 104145.
Chapman, J.B., Ducea, M.N., DeCelles, P.G., Profeta, L., 2015. Tracking changes in crustal thickness during orogenic evolution with Sr/Y: An example from the North American Cordillera. Geology 43, 919–922.
Cheng, C., Li, S., Xie, X., Xie, W., Yang, D., Chai, G., Lu, Y., Wei, X., Li, M., Hu, B., Busbey, A.B., 2024. Crustal thickness variation of the Dabie orogenic belt: Insights from detrital zircon evidence and geological significance. Gondwana Res. 129, 355–366.
Claiborne, L.L., Miller, C.F., Gualda, G.A., Carley, T.L., Covey, A.K., Wooden, J.L., Fleming, M.A., 2018. Zircon as magma monitor: Robust, temperature-dependent partition coefficients from glass and zircon surface and rim measurements from natural systems. Microstruct. Geochronol.: Planet. Rec. Atom Scale, 1–33.
Condie, K.C., Pisarevsky, S.A., Puetz, S.J., Spencer, C.J., Teixeira, W., Faleiros, F.M., 2022a. A reappraisal of the global tectono-magmatic lull at$\sim$ 2.3 Ga. Precambrian Res. 376, 106690.
Condie, K.C., Puetz, S.J., Spencer, C.J., Roberts, N.M.W., 2022b. Secular compositional changes in hydrated mantle: The record of arc-type basalts. Chem. Geol. 607, 121010.
Condie, K.C., Puetz, S.J., Spencer, C.J., Roberts, N.M.W., 2024. Four billion years of secular compositional change in granitoids. Chem. Geol. 644, 121868.
Crisp, L.J., Berry, A.J., Burnham, A.D., Miller, L.A., Newville, M., 2023. The Ti-in-zircon thermometer revised: The effect of pressure on the Ti site in zircon. Geochim. Cosmochim. Acta 360, 241–258. https://doi.org/10.1016/j.gca.2023.04.031.
Dhuime, B., Hawkesworth, C.J., Cawood, P.A., Storey, C.D., 2012. A change in the geodynamics of continental growth 3 billion years ago. Science 335 (6074), 1334–1336.
Dong, L., Bai, X., Song, M., Wang, R., 2023. Crustal thickness of the Jiaodong Peninsula in the Mesozoic: Implications for the destruction of the North China Craton. Front. Earth Sci. 11, 1171456.
Dong, Y., Cao, S., Zhan, L., Li, W., Neubauer, F., Genser, J., 2022. Tectono-magmatism evolution in the Gaoligong orogen belt during Neoproterozoic to Paleozoic: Significance for assembly of East Gondwana. Precambrian Res. 378, 106776.
Ferry, J.M., Watson, E.B., 2007. New thermodynamic models and revised calibrations for the Ti-in-zircon and Zr-in-rutile thermometers. Contrib. Mineral. Petrol. 154 (4), 429–437.
Gard, M., Hasterok, D., Halpin, J.A., 2019. Global whole-rock geochemical database compilation. Earth Syst. Sci. Data 11, 1553–1566.
Grimes, C.B., John, B.E., Kelemen, P.B., Mazdab, F.K., Wooden, J.L., Cheadle, M.J., Hanghøj, K., Schwartz, J.J., 2007. Trace element chemistry of zircons from oceanic crust: A method for distinguishing detrital zircon provenance. Geology 35, 643–646.
Hu, P.Y., Zhai, Q.G., Cawood, P.A., Weinberg, R.F., Zhao, G.C., Tang, Y., Liu, Y.M., 2023a. Paleogeographic reconstruction of Precambrian terranes reworked by Phanerozoic orogens: An example based on detrital zircon REE from Lhasa terrane in southern Tibet. Geophys. Res. Lett. 50 (5), 2023GL102979.
Hu, Y., Zhang, R., Zhang, C., Bai, H., 2023b. Tracking the formation and evolution of the Ordos Block basement, North China Craton: U-Pb age and Lu-Hf isotope record of detrital zircons from the early Mesoproterozoic sandstones. Precambrian Res. 397, 107171.
Ickert, R.B., Williams, I.S., Wyborn, D., 2011. Ti in zircon from the Boggy Plain zoned pluton: implications for zircon petrology and Hadean tectonics. Contrib. Mineral. Petrol. 162, 447–461.
Jaramillo, J.S., Zapata, S., Carvalho, M., Cardona, A., Jaramillo, C., Crowley, J.L., Bayona, G., Caballero-Rodriguez, D., 2022. Diverse magmatic evolutionary trends of the Northern Andes unraveled by Paleocene to early Eocene detrital zircon geochemistry. Geochem. Geophys. Geosyst. 23 (9), 2021GC010113.
Keller, C.B., Schoene, B., 2012. Statistical geochemistry reveals disruption in secular lithospheric evolution about 2.5 Gyr ago. Nature 485, 490–493.
Keller, B., Schoene, B., 2018. Plate tectonics and continental basaltic geochemistry throughout Earth history. Earth Planet. Sci. Lett. 481, 290–304.
Laurent, O., Moyen, J.F., Wotzlaw, J.F., Björnsen, J., Bachmann, O., 2022. Early Earth zircons formed in residual granitic melts produced by tonalite differentiation. Geology 50 (4), 437–441.
Lei, M., Chen, J., Li, C., 2022. Geochemical evidence for the Eocene surface uplift of the southern Lhasa subterrane, southern Tibet and the implications. Lithos 434, 106919.
Li, Y., Gong, C., Peng, G., Qiu, X., Steel, R.J., Xiao, Z., He, Y., Qi, K., Yu, Y., 2023. Detrital zircon signals of the late Eocene provenance change of the Pearl River Mouth Basin, northern South China Sea. Sediment. Geol. 451, 106409.
Liu, X., Gao, R., Guo, X., Ding, L., 2023. Detrital zircon U-Pb geochronology of the Lunpola basin strata constrains the Cenozoic tectonic evolution of central Tibet. Gondwana Res. 113, 179–193.
Liu, H., McKenzie, N.R., Colleps, C.L., Chen, W., Ying, Y., Stockli, L., Sardsud, A., Stockli, D.F., 2022. Zircon isotope–trace element compositions track Paleozoic-Mesozoic slab dynamics and terrane accretion in Southeast Asia. Earth Planet. Sci. Lett. 578, 117298.
Loucks, R.R., Fiorentini, M.L., Rohrlach, B.D., 2018. Divergent T–fO_2 paths during crystallisation of H_2O-rich and H_2O-poor magmas as recorded by Ce and U in zircon, with implications for TitaniQ and TitaniZ geothermometry. Contrib. Mineral. Petrol. 173, 1–21.
Luffi, P., Ducea, M.N., 2022. Chemical mohometry: Assessing crustal thickness of ancient orogens using geochemical and isotopic data. Rev. Geophys. 60, 2021RG000753.
McDonough, W.F., Sun, S.S., 1995. The composition of the Earth. Chem. Geol. 120 (3–4), 223–253.
McKenzie, N.R., Smye, A.J., Hegde, V.S., Stockli, D.F., 2018. Continental growth histories revealed by detrital zircon trace elements: A case study from India. Geology 46, 275–278.
Moghadam, H.S., Li, Q.L., Griffin, W.L., Stern, R.J., Santos, J.F., Ducea, M.N., Ottley, C.J., Karsli, O., Sepidbar, F., O'Reilly, S.Y., 2022. Temporal changes in subduction-to collision-related magmatism in the Neotethyan orogen: The Southeast Iran example. Earth-Sci. Rev. 226, 103930.
Moreira, H., Buzenchi, A., Hawkesworth, C.J., Dhuime, B., 2023. Plumbing the depths of magma crystallization using $^{176}Lu/^{177}Hf$ in zircon as a pressure proxy. Geology 51 (3), 233–237. https://doi.org/10.1130/G50659.1.
Paulsen, T., Deering, C., Sliwinski, J., Chatterjee, S., Bachmann, O., Guillong, M., 2021. Crustal thickness, rift-drift and potential links to key global events. Terra Nova 33, 12–20.
Paulsen, T., Deering, C., Sliwinski, J., Chatterjee, S., Bachmann, O., 2022. Continental magmatism and uplift as the primary driver for first-order oceanic $^{87}Sr/^{86}Sr$ variability with implications for global climate and atmospheric oxygenation. GSA Today 32, 4–10.
Pereira, I., van Schijndel, V., Tedeschi, M., Cutts, K., Guitreau, M., 2024. A review of detrital heavy mineral contributions to furthering our understanding of continental crust formation and evolution. Geol. Soc. Lond. Special Publ. 537 (1), 9–55.
Profeta, L., Ducea, M.N., Chapman, J.B., Paterson, S.R., Gonzales, S.M.H., Kirsch, M., Petrescu, L., DeCelles, P.G., 2015. Quantifying crustal thickness over time in magmatic arcs. Sci. Rep. 5, 1–7.
Puetz, S.J., Spencer, C.J., Ganade, C.E., 2021. Analyses from a validated global UPb detrital zircon database: enhanced methods for filtering discordant UPb zircon analyses and optimizing crystallization age estimates. Earth-Sci. Rev. 220, 103745.
Reimink, J.R., Davies, J.H., Bauer, A.M., Chacko, T., 2020. A comparison between zircons from the Acasta Gneiss Complex and the Jack Hills region. Earth Planet. Sci. Lett. 531, 115975.
Roberts, N.M.W., Condie, K.C., Palin, R.M., Spencer, C.J., 2023. Hot, wide, continental back-arcs explain Earth's enigmatic mid-Proterozoic magmatic and metamorphic record. Tektonika 1 (1), 67–75. https://doi.org/10.55575/tektonika2023.1.1.32.
Roberts, N.M.W., Hernández-Montenegro, J.D., Palin, R.M., 2024. Garnet stability during crustal melting: Implications for chemical mohometry and secular change in arc magmatism and continent formation. Chem. Geol. 659, 122142. https://doi.org/10.1016/j.chemgeo.2024.122142.
Roberts, N.M.W., Spencer, C.J., 2015. The zircon archive of continent formation through time. Geol. Soc. Lond. Special Publ. 389, 197–225. https://doi.org/10.1144/SP389.1.
Schiller, D., Finger, F., 2019. Application of Ti-in-zircon thermometry to granite studies: problems and possible solutions. Contrib. Mineral. Petrol. 174, 1–16.
Spencer, C.J., Hawkesworth, C., Cawood, P.A., Dhuime, B., 2013. Not all supercontinents are created equal: Gondwana-Rodinia case study. Geology 41, 795–798.
Sundell, K.E., Laskowski, A.K., Howlett, C., Kapp, P., Ducea, M., Chapman, J.B., Ding, L., 2024. Episodic Late Cretaceous to Neogene crustal thickness variation in southern Tibet. Terra Nova 36 (1), 45–52.
Sundell, K.E., Macdonald, F.A., 2022. The tectonic context of hafnium isotopes in zircon. Earth Planet. Sci. Lett. 584, 117426.
Tamblyn, R., Hasterok, D., Hand, M., Gard, M., 2022. Mantle heating at ca. 2 Ga by continental insulation: Evidence from granites and eclogites. Geology 50, 91–95.
Tang, M., Ji, W.Q., Chu, X., Wu, A., Chen, C., 2021a. Reconstructing crustal thickness evolution from europium anomalies in detrital zircons. Geology 49, 76–80.
Tang, M., Chu, X., Hao, J., Shen, B., 2021b. Orogenic quiescence in Earth's middle age. Science 371, 728–731.
Trail, D., Watson, E.B., Tailby, N.D., 2012. Ce and Eu anomalies in zircon as proxies for the oxidation state of magmas. Geochim. Cosmochim. Acta 97, 70–87.
Triantafyllou, A., Ducea, M.N., Jepson, G., Hernández-Montenegro, J.D., Bisch, A., Ganne, J., 2023. Europium anomalies in detrital zircons record major transitions in Earth geodynamics at 2.5 Ga and 0.9 Ga. Geology 51 (2), 141–145. https://doi.org/10.1130/G50720.1.
Verdel, C., Campbell, M.J., Allen, C.M., 2021. Detrital zircon petrochronology of central Australia, and implications for the secular record of zircon trace element composition. Geosphere 17, 538–560.
Wang, Z., Wang, Z., Zhang, Y., Xu, B., Li, Y., Tian, Y., Wang, Y., Peng, J., 2022. Linking $\sim$1.4–0.8 Ga volcano-sedimentary records in eastern Central Asian orogenic belt

with southern Laurentia in supercontinent cycles. Gondwana Res. 105, 416–431.
Watson, E.B., Wark, D.A., Thomas, J.B., 2006. Crystallization thermometers for zircon and rutile. Contrib. Mineral. Petrol. 151 (4), 413–433.
Wu, G.H., Chu, X., Tang, M., Li, W., Chen, F., 2023. Distinct tectono-magmatism on the margins of Rodinia and Gondwana. Earth Planet. Sci. Lett. 609, 118099.
Xiong, L., Song, S., Su, L., Zhang, G., Allen, M.B., Feng, D., Yang, S., 2023. Detrital zircons from high-pressure trench sediments (Qilian Orogen): constraints on continental-arc accretion, subduction initiation and polarity of the Proto-Tethys Ocean. Gondwana Res. 113, 194–209.
Yakymchuk, C., Holder, R.M., Kendrick, J., Moyen, J.F., 2023. Europium anomalies in zircon: A signal of crustal depth? Earth Planet. Sci. Lett. 622, 118405.
Zeng, Y.C., Xu, J.F., Chen, J.L., Wang, B.D., Huang, F., 2022. How and how much did Western Central Tibet raise by India-Asia collision? Geophys. Res. Lett. 49 (20), 2022GL101206.
Zhang, Z.J., Kusky, T., Gao, M., Cheng, Q.M., 2023. Spatio-temporal analysis of big data sets of detrital zircon U-Pb geochronology and Hf isotope data: Tests of tectonic models for the Precambrian evolution of the North China Craton. Earth-Sci. Rev. 239, 104372. https://doi.org/10.1016/j.earscirev.2023.104372.
Zhong, S., Li, S., Seltmann, R., Lai, Z., Zhou, J., 2021. The influence of fractionation of REE-enriched minerals on the zircon partition coefficients. Geosci. Front. 12, 101094.